A measurement of the proton plus helium spectrum of cosmic rays in the TeV region with HAWC

J. C. Arteaga-Velázquez[1⋆] on behalf of the HAWC collaboration

1 Instituto de Física y Matemáticas, Universidad Michoacana de San Nicolás de Hidalgo, 58040 Morelia, Mexico

⋆ juan.arteaga@umich.mx

A complete list of HAWC's authors is available at:
https://www.hawc-observatory.org/collaboration/

Abstract

HAWC is an air-shower detector designed to study TeV gamma and cosmic rays. The observatory is composed of a $22000\,m^2$ array of 300 water Cherenkov tanks ($4.5\,m$ deep x $7.3\,m$ diameter) with 4 photomultipliers (PMT) each. The instrument registers the number of hit PMTs, the timing information and the total charge at the PMTs during the event. From these data, shower observables such as the arrival direction, the core position at ground, the lateral age and the primary energy are estimated. In this work, we study the distribution of the shower age vs the primary energy of a sample of shower data collected by HAWC from June 2015 to June 2019 and employ a shower-age cut based on predictions of QGSJET-II-04 to separate a subsample of events dominated by H and He primaries. Using these data and a dedicated analysis, we reconstruct the cosmic ray spectrum of H+He from 6 to 158 TeV, which shows the presence of a softening at around 24 TeV with a statistical significance of 4.1σ.

1 Introduction

The $10-100$ TeV energy region of the cosmic-ray energy spectrum has been recently the target of both direct and indirect experiments due to the lack of in-depth studies on the composition and spectrum of cosmic-ray particles in this energy range. This was mainly the result of experimental limitations of direct and indirect detection techniques. Recent progress on the matter has allowed to overcome such constraints allowing to boost detailed studies on the properties

of such particles. As an example, on the side of indirect cosmic-ray detection, we have some recent studies from HAWC on the energy spectrum and composition of cosmic rays at tens of TeV [1, 2]. Composition measurements of cosmic rays from 10 TeV to 100 TeV with extensive air-shower (EAS) experiments are scarce. Just a few EAS experiments have reported data on cosmic-ray composition in this energy regime. In particular, ARGO-YBJ performed measurements on the spectrum of the H+He mass group [3, 4], EAS-TOP with MACRO, on the intensity of H, He and CNO primaries [5], KASCADE, on the flux of p primaries [6], MAGIC, on the intensity of protons [7], and HESS [8] and VERITAS [9], on the spectrum of Fe nuclei. Now, HAWC has joined these efforts with a measurement of the cosmic-ray spectrum of H+He between 6 and 158 TeV [2]. In this work, we will present a brief description of this analysis. The procedure is simple: we selected a subsample of HAWC events enriched with H and He nuclei based on a cut on the shower age that is derived from MC simulations using FLUKA/QGSJET-II-04. Then, we unfolded the energy distribution of the data subsample and, finally, we corrected it for the contamination of heavy elements ($Z > 2$) and for losses in the trigger and reconstruction efficiency. With MC studies, we found that the H+He mass group can be easily separated with this procedure due to its large relative abundance in the energy interval from 10 to 100 TeV. For this reason, we selected this group for the analysis. More details and discussions about this study and its results can be found in [2].

2 HAWC observatory, data and simulations

HAWC is an air-shower Cherenkov detector dedicated to measure gamma and cosmic rays in the energy interval from 100 GeV up to 100 TeV, and even up to 1 PeV in case of cosmic-ray primaries. It is located in the east-central part of Mexico, at an altitude of 4100 m at the Sierra Negra Volcano [10]. The HAWC central detector is composed of an array of 300 water Cherenkov detectors (7.3 m diameter × 4.5 m deep), which covers a surface of 22000 m^2. Each of these detector units has 4 PMTs, which provide data on the arrival times and the effective charge of the front of EAS events. From these measurements a dedicated reconstruction program estimates different air shower observables as the core location, arrival direction, the lateral shower profile, among others [10, 11]. For this study, of particular interest are the lateral shower age s and the estimated primary energy E_{rec} of the event. The shower age is obtained event by event from a χ^2 fit with a Nishimura-Kamata-Greisen (NKG) like function to the measured lateral charge distribution [11]. On the other hand, the primary energy is estimated with a maximum likelihood procedure that compares the observed lateral charge profile with Monte Carlo (MC) templates for the lateral charge distributions [1]. The templates were produced with CORSIKA [12] and the hadronic interaction models FLUKA [13] and QGSJET-II-04 [14] using proton-induced showers and different zenith angle and energy bins, which cover the zenith angle interval $\theta < 60°$ and the primary energy range $E = 70\,\text{GeV} - 1.4\,\text{PeV}$, respectively.

For the present analysis, we employed HAWC data collected between June 11, 2015 to June 3, 2019, corresponding to an effective time of $T_{eff} = 3.74$ years. To reduce the systematic errors in our study, we applied the following data selection criteria: we employed showers with zenith angles smaller than $\sim 16.7°$, which were successfully reconstructed, that activated at least 40 PMTs within a radius of 40 m from the shower core, which exhibited a fraction of hit PMTs greater or equal 0.2 and reconstructed energy in the interval $\log_{10}(E_{rec}/\text{GeV}) = [3.5, 5.5]$. These cuts were also used on our MC simulations.

The MC data sets for our analysis were produced with CORSIKA using FLUKA and QGSJET-II-04 for hadronic energies $< 80\,\text{GeV}$ and $\geq 80\,\text{GeV}$, respectively. We simulated eight primary nuclei (H, He, C, O, Ne, Mg, Si, Fe) with energies from 5 GeV to 3 PeV and an E^{-2} spectrum,

which were weighted to follow broken-power law spectra [1, 2] that were fit to data from AMS-2 [15], CREAM [16] and PAMELA [17].

After selection cuts, we kept 1.6×10^{10} showers in the measured data set and 3.43×10^5 events in the MC simulations. Above 10 TeV, using our MC data set, we estimated that the selected data sample has energy (in logarithmic scale) and core resolutions smaller than 0.26 and 15 m, respectively, and a pointing resolution better than 0.55°.

3 Analysis procedure

To start the analysis, we applied an energy-dependent cut on the lateral shower age to select a subsample of events dominated by protons and helium primaries. Using our MC simulations, we put the cut between the mean predictions for He and C nuclei and we only kept young EAS with s values smaller than this cut, as such events are most likely produced by H and He primaries. The MC predictions for the mean shower age of EAS induced by different primary nuclei are shown in the left plot of Fig. 1 as a function of the reconstructed energy. The shower-age cut applied on the analysis is also displayed. From MC simulations and our nominal composition model, the purity of the subsample is expected to be greater than 82% in each bin of E_{rec} using our selection criterion. The energy histogram of the experimental data sample after applying the shower cut is shown on the right plot of Fig. 1. It is compared with the energy histogram before applying the age cut on the selected data.

The subsample of young EAS has almost 9.9×10^9 events and its histogram is not corrected for migration effects yet. For this reason, we applied the method of Bayesian unfolding [18]. The iteration depth was set at the minimum of the Weighted Mean Squared Error [19]. The prior distribution was calculated from the spectrum for the H+He intensity in our nominal composition model. In addition, in every intermediate step during the unfolding procedure, but excluding the last one, we smoothed the energy spectrum using a fit with a broken power-
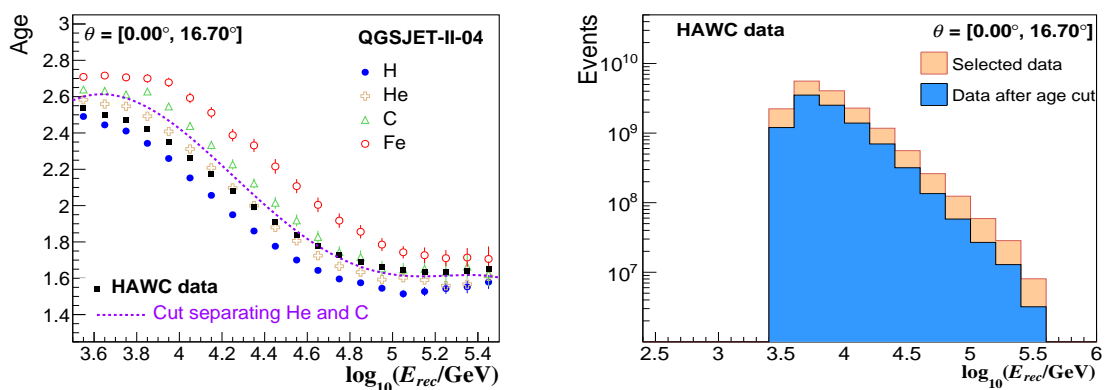
Figure 1: Left: FLUKA/QGSJET-II-04 predictions for the mean shower age vs the reconstructed primary energy of different cosmic-ray nuclei: H (filled circles), He (crosses), C (triangles) and Fe (open circles). The segmented line represents the shower-age cut used for the selection of our subsample of young showers for the analysis. The mean shower age for HAWC data is shown with squares [2]. Right: The raw energy histogram for the data after applying quality cuts (orange) is compared with the corresponding histogram for the subsample of young EAS obtained after using the shower-age cut [2].
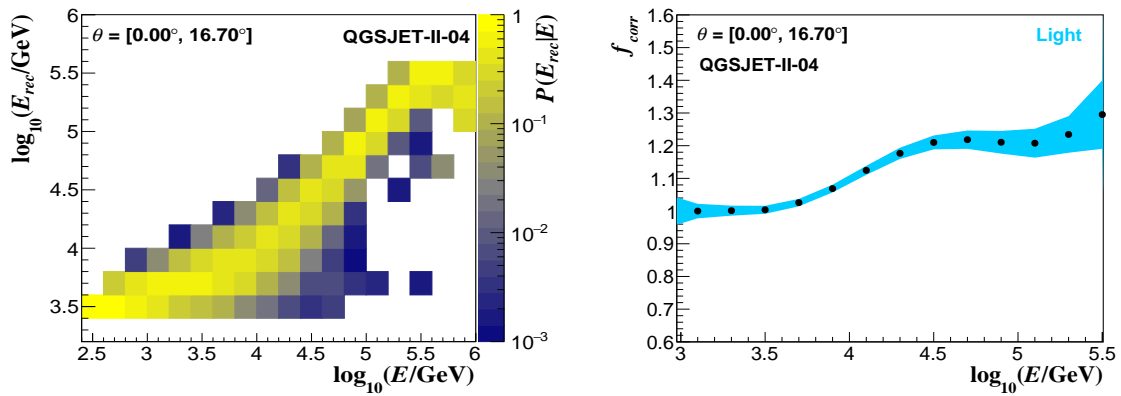
Figure 2: Left: The response matrix for the subsample of young EAS calculated with QGSJET-II-04 and our cosmic-ray composition model [2]. Right: f_{corr} vs the true primary energy E according to MC simulations. The error band represents statistical uncertainties [2].

law function [20]. The response matrix employed for unfolding the raw energy distribution was obtained using MC simulations and our nominal composition model (see left plot of Fig. 2).

In a next step, we calculated a factor f_{corr} to correct the unfolded result $N(E)$ for the contamination of heavy elements (c.f. right plot of Fig. 2). This quantity is computed from MC simulations for different true energy (E) bins as the inverse of the proportion of H and He nuclei in the subsample of young showers. Then, to correct for losses of trigger and reconstruction efficiency, we calculated the effective area for the H+He mass group A_{eff}^{H+He} with MC simulations using our nominal composition model as a function of E (see left plot of Fig. 3). Finally, the energy spectrum of H+He nuclei was estimated as

$$\Phi(E) = \frac{N(E)}{\Delta E \, T_{eff} \, \Delta\Omega \, f_{corr}(E) \, A_{eff}^{H+He}(E)}, \tag{1}$$

where $\Delta\Omega = 0.27\,\text{sr}$ is the solid-angle interval of observation.

4 Results

The energy spectrum of H+He nuclei is shown in the right plot of Fig. 3 along with its statistical and systematic errors. Inside the interval $\log_{10}(E/\text{GeV}) = [3.8, 5.2]$, statistical errors are smaller than 3.8%. They include the statistical uncertainties due to the limited statistics of the MC simulations and the statistics of the measured data, both added in quadrature. On the other hand, systematic errors are found within -22.6% and $+28.9\%$. They incorporate uncertainties from the modelling of the PMTs, the high-energy hadronic interaction model (for which we also used EPOS-LHC [21] simulations), the relative abundances of cosmic rays (we employed the Polygonato model [22], three additional composition models calibrated with direct data from ATIC-2 [23], JACEE [24] and MUBEE [25], respectively, and an additional model for which we varied the intensity of the heavy component in our nominal composition model to match the observed abundance of heavy primaries from an analysis of the efficiency of the shower-age cut [2]), the seed spectrum in the unfolding procedure (changing the prior spectrum by uniform and $E^{-1.5}$ distributions), the method of unfolding (using also the Gold's algorithm [26]), the smoothing procedure (employing a fit with a 5th degree polynomial and
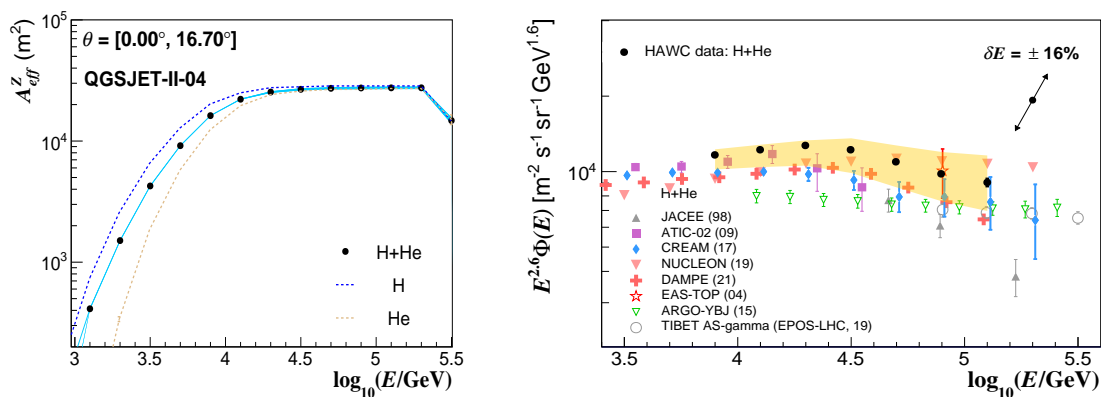
Figure 3: Left: The effective area for H+He primaries (data points) as a function of the true primary energy as estimated with MC simulations [2]. It is compared with the effective area expected for pure protons (blue dashed line) and He nuclei (orange dashed line). Statistical uncertainties are shown with an error band. Right: The energy spectrum of H+He cosmic rays as measured with HAWC (black data points) in comparison with TeV measurements of the same mass group from direct and indirect cosmic-ray experiments [2] (see text for a description). The error band for HAWC data represents the systematic uncertainties, while the vertical error bars, statistical errors. For the other data points, only statistical errors are displayed.

the 353HQ-twice algorithm [27] of ROOT [28], respectively), the corrected effective area and the position of the shower-age cut (putting the cut at the curves for the mean age of He and C primaries, respectively). The largest contributions to the systematic error are due to uncertainties in the PMT modelling (it is found within $-10.6\%/+28.5\%$), the high-energy hadronic interaction model (it contributes with an error between -10.9% and -3.7%) and the cosmic-ray composition (with errors between -17.3% and $+2.1\%$). The sum in quadrature of the remaining uncertainty sources ranges from -7% to $+5.2\%$. In all cases the shape of the spectrum is preserved.

In the spectrum of HAWC for H+He nuclei, we observe the presence of a break at some tens of TeV. A fit of the spectrum with a broken power-law expression [20]

$$\Phi(E) = \Phi_0 E^{\gamma_1}\left[1+\left(\frac{E}{E_0}\right)^\varepsilon\right]^{(\gamma_2-\gamma_1)/\varepsilon}, \tag{2}$$

shows the existence of a softening at around $E_0 = 24.0^{+3.6}_{-3.1}$ TeV associated with a change in the spectral index from $\gamma_1 = -2.51 \pm 0.02$ to $\gamma_2 = -2.83 \pm 0.02$. The fit gave a chi-squared $\chi^2 = 0.26$ for 2 degrees of freedom. A statistical analysis based on the difference between the χ^2 of this fit with that obtained with a power-law formula as a test statistics yielded a statistical significance of 4.1σ for the feature [2].

To end, the HAWC result is compared with measurements of direct and other indirect cosmic-ray experiments in the TeV energy range in the right plot of Fig. 3. We observe that HAWC results confirm previous hints from ATIC-2 [29], CREAM I-III [30] and NUCLEON [31] about the existence of a break in the spectrum of H+He cosmic rays at tens of TeV. This result is also strengthen by recent DAMPE data [32]. We also see that our result is in agreement with ATIC-2 and NUCLEON within systematic uncertainties, but it seems to be above DAMPE (at low energies) and CREAM data. The HAWC spectrum is also above the ARGO-YBJ [4] and TIBET AS$-\gamma$ [33] measurements, but in agreement with EAS-TOP data [5].

5 Conclusion

A dedicated analysis of cosmic ray composition with HAWC has allowed to measure the spectrum of H+He of cosmic rays in the energy range $E = [6, 158]$ TeV. The spectrum shows a softening at $24.0^{+3.6}_{-3.1}$ TeV with a statistical significance of $4.1\,\sigma$. This analysis shows the potential of high-altitude water Cherenkov observatories like HAWC for composition studies of cosmic rays.

Acknowledgements

The main list of acknowledgements can be found under the following link: https://www.hawc-observatory.org/collaboration. In addition, J.C.A.V. also wants to thank the partial support from CONACYT grant A1-S-46288 and the Coordinación de la Investigación Científica de la Universidad Michoacana.

References

[1] R. Alfaro, HAWC collaboration, *All-particle cosmic ray energy spectrum measured by the HAWC experiment from 10 to 500 TeV*, Phys. Rev. D **96**, 122001 (2017), doi:10.1103/PhysRevD.96.122001.

[2] A. Albert et al., *Cosmic ray spectrum of protons plus helium nuclei between 6 and 158 TeV from HAWC data*, Phys. Rev. D **105**, 063021 (2022), doi:10.1103/PhysRevD.105.063021.

[3] B. Bartoli, ARGO-YBJ Collaboration, *Light-component spectrum of the primary cosmic rays in the multi-TeV region measured by the ARGO-YBJ experiment*, Phys. Rev. D **85**, 092005 (2012), doi:10.1103/PhysRevD.85.092005.

[4] B. Bartoli, ARGO-YBJ Collaboration, *Cosmic ray proton plus helium energy spectrum measured by the ARGO-YBJ experiment in the energy range 3-300 TeV*, Phys. Rev. D **91**, 112017 (2015), doi:10.1103/PhysRevD.91.112017.

[5] M. Aglietta et al., *The cosmic ray proton, helium and CNO fluxes in the 100 TeV energy region from TeV muons and EAS atmospheric Cherenkov light observations of MACRO and EAS-TOP*, Astropart. Phys. **21**, 223 (2004), doi:10.1016/j.astropartphys.2004.01.005.

[6] T. Antoni et al., *The primary proton spectrum of cosmic rays measured with single hadrons at ground level*, Astrophys. J. **612**, 914 (2004), doi:10.1086/422674.

[7] P. Temnikov et al., *Protons spectrum from MAGIC telescopes data*, Proc. Sci. **395**, 231 (2021), doi:10.22323/1.395.0231.

[8] F. Aharonian et al., *First ground-based measurement of atmospheric Cherenkov light from cosmic rays*, Phys. Rev. D **75**, 042004 (2007), doi:10.1103/PhysRevD.75.042004.

[9] A. Archer et al., *Measurement of the iron spectrum in cosmic rays by VERITAS*, Phys. Rev. D **98**, 022009 (2018), doi:10.1103/PhysRevD.98.022009.

[10] A. U. Abeysekara et al., *Observation of the Crab Nebula with the HAWC Gamma-Ray Observatory*, Astrophys. J. **843**, 39 (2017), doi:10.3847/1538-4357/aa7555.

[11] A. U. Abeysekara et al., *Measurement of the Crab Nebula spectrum past 100 TeV with HAWC*, Astrophys. J. **881**, 134 (2019), doi:10.3847/1538-4357/ab2f7d.

[12] D. Heck, J. Knapp, J. N. Capdevielle, G. Schatz and T. Thouw, *CORSIKA: A Monte Carlo Code to Simulate Extensive Air Showers*, Report FZKA-6019 (1998).

[13] G. Battistoni, F. Cerutti, A. Fasso, A. Ferrari, S. Muraro, J. Ranft, S. Roesler and P. R. Sala, *The FLUKA code: description and benchmarking*, AIP Conf. Proc. **896**, 31 (2007), doi:10.1063/1.2720455.

[14] S. Ostapchenko, *Monte Carlo treatment of hadronic interactions in enhanced Pomeron scheme: QGSJET-II model*, Phys. Rev. D **83**, 014018 (2011), doi:10.1103/PhysRevD.83.014018.

[15] M. Aguilar et al., *Precision measurement of the helium flux in primary cosmic rays of rigidities 1.9 GV to 3 TV with the alpha magnetic spectrometer on the International Space Station*, Phys. Rev. Lett. **115**, 211101 (2015), doi:10.1103/PhysRevLett.115.211101.

[16] Y. Yoon, CREAM collaboration, *Cosmic-ray proton and helium spectra from the first cream flight*, Astrophys. J. **728**, 122 (2011), doi:10.1088/0004-637X/728/2/122.

[17] O. Adriani, PAMELA collaboration, *PAMELA measurements of cosmic-ray proton and helium spectra*, Science **332**, 69 (2011), doi:10.1126/science.1199172.

[18] G. D'Agostini, *A multidimensional unfolding method based on Bayes' theorem*, Nucl. Instrum. Methods Phys. Res. A: Accel. Spectrom. Detect. Assoc. Equip. **362**, 487 (1995), doi:10.1016/0168-9002(95)00274-X.

[19] T. Antoni et al., *KASCADE measurements of energy spectra for elemental groups of cosmic rays: Results and open problems*, Astropart. Phys. **24**, 1 (2005), doi:10.1016/j.astropartphys.2005.04.001.

[20] S. V. Ter-Antonyan and L. S. Haroyan, *About EAS size spectra and primary energy spectra in the knee region*, (arXiv preprint) doi:10.48550/arXiv.hep-ex/0003006.

[21] T. Pierog, Iu. Karpenko, J. M. Katzy, E. Yatsenko and K. Werner, *EPOS LHC: Test of collective hadronization with data measured at the CERN Large Hadron Collider*, Phys. Rev. C **92**, 034906 (2015), doi:10.1103/PhysRevC.92.034906.

[22] J. R. Hörandel, *On the knee in the energy spectrum of cosmic rays*, Astropart. Phys. **19**, 193 (2003), doi:10.1016/S0927-6505(02)00198-6.

[23] A. D. Panov et al., *Elemental energy spectra of cosmic rays from the data of the ATIC-2 experiment*, Bull. Russ. Acad. Sci. Phys. **71**, 494 (2007), doi:10.3103/S1062873807040168.

[24] Y. Takahashi, *Elemental abundance of high energy cosmic rays*, Nucl. Phys. B, Proc. Suppl. **60**, 83 (1998), doi:10.1016/S0920-5632(97)00503-3.

[25] V. I. Zatsepin, MUBEE Collaboration, *Energy spectra and composition of primary cosmic rays above 10 eV*, In D. A. Leahy, R. B. Hickws and D. Venkatesan, eds., Proceedings of the 23rd ICRC, Calgary, Canada (1993).

[26] R. Gold, *An iterative unfolding method for response matrices*, Report No ANL-6984 (1964).

[27] J. Friedman, *Data analysis techniques for high energy particle physics*, In Proceedings of the 3rd CERN School of Computing (Norway), CERN, Geneva, p. 271 (1974).

[28] R. Brun and F. Rademakers, *ROOT — An object oriented data analysis framework*, Nucl. Instr. Meth. Phys. Res. A **389**, 81 (1997), doi:10.1016/S0168-9002(97)00048-X.

[29] A. D. Panov et al., *Energy spectra of abundant nuclei of primary cosmic rays from the data of ATIC-2 experiment: Final results*, Bull. Russ. Acad. Sci. Phys. **73**, 564 (2009), doi:10.3103/S1062873809050098.

[30] Y. S. Yoon et al., *Proton and Helium Spectra from the CREAM-III Flight*, Astrophys. J. **839**, 5 (2017), doi:10.3847/1538-4357/aa68e4.

[31] E. V. Atkin et al., *Energy Spectra of Cosmic-Ray Protons and Nuclei Measured in the NUCLEON Experiment Using a New Method*, Astron. Rep. **63**, 66 (2019), doi:10.1134/S1063772919010013.

[32] F. Alemanno et al., *Measurement of the light component (p+He) energy spectrum with the DAMPE space mission*, Proc. Sci. **395**, 117 (2021), doi:10.22323/1.395.0117.

[33] M. Amenomori, *The cosmic ray energy spectrum measured with the new Tibet hybrid experiment*, EPJ Web Conf. **208**, 03001 (2019), doi:10.1051/epjconf/201920803001.